Optical properties of Tl²⁺ hole centres in alkali halides: II. MS-Xα calculations

Optical properties of Tl^{2+} hole centres in alkali halides: II. MS–Xα calculations

I Cabria†, M Moreno†, J A Aramburu†, M T Barriuso‡, U Rogulis§‖ and J-M Spaeth§

† Departamento Ciencias de la Tierra y Física de la Materia Condensada, Facultad de Ciencias, Universidad de Cantabria, 39005 Santander, Spain
‡ Departamento Física Moderna, Facultad de Ciencias, Universidad de Cantabria, 39005 Santander, Spain
§ Universität-Gesamthochschule Paderborn, Fachbereich Physik, Warburger Strasse 100, D-33098 Paderborn, Germany

Abstract. MS–Xα calculations at different values of the metal–ligand distance, R, have been performed for TlX$_6^{4-}$ units (X = Cl, Br, I) subjected to the electrostatic potential of KX lattices. The results confirm that the optical absorption bands peaked at 3.4 and 4.2 eV in KCl:Tl^{2+} can be associated with the $t_{1u}(\pi) \rightarrow a_{1g}^*$ and $t_{1u}(\sigma) \rightarrow a_{1g}^*$ charge transfer (CT) transitions respectively of the TlCl$_6^{4-}$ complex. Also, the systematic red shift experienced by such transitions on passing from KX to RbX is related to the increase of R induced by the host lattice change. The spin–orbit coupling in $t_{1u}(\pi)$ and $t_{1u}(\sigma)$ levels determines the sign of the magnetic circular dichroism of the optical absorption (MCDA) and it is shown that for bromides and iodides the two CT transitions can exhibit a different pattern as is experimentally observed. Also the non-existence of MCDA signal in the $t_{1u}(\sigma) \rightarrow a_{1g}^*$ region of KCl:Tl^{2+} is related to a practically zero value of the spin–orbit splitting. The existence of five CT peaks for iodides is explained through the γ_{8-} component of the $t_{2u} \rightarrow a_{1g}^*$ CT transition, whose oscillator strength increases following the ligand spin–orbit coefficient. As t_{2u} is always found to be located about 0.15 eV below $t_{1u}(\pi)$, this new component can also explain the asymmetry observed in the MCDA spectra of chlorides and bromides in the high energy side of the $t_{1u}(\pi) \rightarrow a_{1g}^*$ transition. In all these TlX$_6^{4-}$ units, the unpaired electron is found to be located mainly on the X ligands, the charge on them increasing along the Cl $\rightarrow$ Br $\rightarrow$ I series. This is related to the corresponding decrease of the hyperfine constant for whose core polarization effects are calculated to be negligible. From the present results, the equilibrium Tl^{2+}–Cl$^-$ distance would be close to 2.80 Å thus implying a 10% inwards relaxation with respect to the host lattice. To our knowledge these are the first calculations reported on heavy 6s^1 impurities.

1. Introduction

Measurements of the magnetic circular dichroism of the optical absorption (MCDA) and the optically detected electron paramagnetic resonance (ODEPR) have been carried out on Tl^{2+} placed in the six KX and RbX lattices (X = Cl, Br, I). The experimental results are reported in part I of the paper (Rogulis *et al* 1998). The measurement of tagged MCDA spectra is relevant as it allows one to associate *unambiguously* the fine details observed through

‖ Permanent address: Institute of Solid State Physics, University of Latvia, 8, Kengaraga Street, LV-1063 Riga, Latvia.

the MCDA technique with a centre well distinguished from others using EPR (Spaeth *et al* 1992). Therefore, a reasonable explanation of the main features displayed by the MCDA spectra clearly ascribed to Tl^{2+} (Rogulis *et al* 1996, 1998) is now attractive and, at the same time, necessary.

Apart from discussing the charge transfer (CT) origin proposed for the lowest bands in $KCl:Tl^{2+}$ (Moreno 1979) and exploring the influence of *ligand* spin–orbit coupling upon the MCDA spectra of the whole series, special attention has to be paid to explain the following experimental facts:

(i) the *red shift* undergone by the first two bands on passing from $KX:Tl^{2+}$ to $RbX:Tl^{2+}$;

(ii) the sign of the circular dichroism for each of the involved bands;

(iii) the absence of MCDA signals for the absorption band peaked at 4.22 eV in $KCl:Tl^{2+}$;

(iv) the existence of five bands in the iodides other than the two transitions coming from the atomic $6s \rightarrow 6p$ ($^2P_{3/2}$; $^2P_{1/2}$) transitions and

(v) the asymmetry of the MCDA spectra in the first absorption band of chlorides and bromides.

To gain a better insight into these problems, theoretical calculations on TlX_6^{4-} complexes (X = Cl, Br, I) placed in alkali halide lattices can be helpful. It is worth noting, for instance, that the first assignments of optical bands due to Tl^{2+}, Ag^0 or Pb^{3+} in alkali halides were made (Moreno 1979) using *only* the empirical optical electronegativity scale (Jørgensen 1970). Moreover, at variance with what is found for 3d impurities, little theoretical effort has been devoted up to now to understand the properties due to s^1 ions (Nistor *et al* 1994). Theoretical calculations have recently been carried out for Ag^0-doped KCl (Cabria *et al* 1997), while calculations on $6s^1$ ions (like Hg^+, Tl^{2+} or Pb^{3+}) placed in insulators have not yet been reported.

For the first calculation of Tl^{2+} in halides the relatively simple MS–$X\alpha$ method was used as this method reasonably explains the charge transfer (CT) bands due to impurities like Cr^{3+} or Cu^{2+} placed in insulators (Aramburu *et al* 1996, Aramburu and Moreno 1997). Moreover, in the case of the $5s^1$-Ag^0-atom-doped KCl, MS–$X\alpha$ and self-consistent charge extended Hückel calculations both have confirmed (Cabria *et al* 1997) the existence of a CT band in the ultraviolet region associated with the Ag^0 impurity.

Relevant details about the calculations are given in the next section, while in section 3 the present theoretical results are used for achieving a better insight into the experimental data of part I.

2. Computational details

In order to explain the *main trends* displayed by the experimental data on Tl^{2+} impurities in six alkali halides, MS–$X\alpha$ calculations have been done for Tl^{2+} embedded in KX lattices (X = Cl, Br, I). Initially, calculations were done on TlX_6^{4-} units subjected to the electrostatic potential due to the rest of the lattice (Aramburu and Moreno 1997). Later, clusters like $(TlX_6K_{12}X_8)^0$ involving 27 ions have been used. As the main features are reproduced by both types of calculation, only the results on seven ion clusters are exposed.

To evaluate the importance of the core polarization contribution to the hyperfine constant, A, polarized MS–$X\alpha$ calculations have also been carried out. As Tl^{2+} is a heavy ion the present MS–$X\alpha$ calculations have been done including all relativistic corrections which are spin independent (Sakurai 1967, Wood and Boring 1978). The influence of spin–orbit coupling on relevant features displayed by optical and MCDA spectra is considered later.

As the equilibrium Tl^{2+}–X^- distance in the different host lattices is not experimentally known, the calculations have been performed at different values of the Tl^{2+}–X^- distance, called R. Taking into account the ionic radii of Pb^{2+} and Hg^{2+} we have tentatively varied R in the range 2.80 Å–3.00 Å for KCl:Tl^{2+} and around 3.0 Å and 3.25 Å for KBr:Tl^{2+} and KI:Tl^{2+}, respectively.

Similar to the procedure employed in previous work (Aramburu *et al* 1992, 1996) atomic sphere radii were chosen following Norman's criterion (Norman 1976) and the α values in the atomic regions taken from Schwarz (1972). Transition energies were considered through the Slater transition state procedure (Slater 1974).

3. Results and discussion

The ordering of significant one-electron orbitals in the ground state of TlX_6^{4-} units is depicted in figure 1. In all these calculations the unpaired electron is found to lie in the antibonding a_{1g}^* level partially related to the 6s level of free Tl^{2+}. A population analysis of this relevant level is presented later.

For testing the importance of relativistic corrections in the present results, firstly the value of the $5d \rightarrow a_{1g}^*$ transition corresponding to the $TlCl_6^{4-}$ complex was explored. When ignoring the relativistic corrections the value of such a transition is calculated to be 14.3 eV, while it becomes equal only to 11.7 eV when including the corrections. This result implies that also this transition is far beyond the optical region and is thus unimportant for the absorption in the optical range. The suppression of relativistic corrections also leads to changes of other properties like the charge distribution in the antibonding a_{1g}^* orbital.

When ignoring in a first approximation the spin–orbit coupling, only the three $a_{1g}^* \rightarrow t_{1u}^*$, $t_{1u}(\pi) \rightarrow a_{1g}^*$ and $t_{1u}(\sigma) \rightarrow a_{1g}^*$ transitions (described in figure 1) are compatible with electric dipole selection rules in O_h symmetry and the Pauli principle. The calculated energy of such transitions for $TlCl_6^{4-}$ is given in table 1. The results given therein strongly support that for KCl:Tl^{2+}, where the optical absorption bands peak at 3.40 eV and 4.22 eV, those transitions can in fact be associated with the CT transitions $t_{1u}(\pi) \rightarrow a_{1g}^*$ and $t_{1u}(\sigma) \rightarrow a_{1g}^*$ of the $TlCl_6^{4-}$ complex. This situation is thus rather different from that calculated at $R = 3.14$ Å for Tl^+ in KCl (Bramanti *et al* 1971) where the separation between $t_{1u}(\sigma)$ and a_{1g}^* levels was found to be 6.5 eV.

As has been found for Cu^{2+} or Cr^{3+} impurities in halides (Aramburu *et al* 1992, 1996) the energy (E) of CT transitions appears to be rather sensitive to changes in R. From table 1 $dE/dR \simeq -70$ meV pm^{-1} is found for both CT transitions of the $TlCl_6^{4-}$ complex. Using this figure, the 0.20 eV red shift experienced by the lowest CT transition on going from KCl:Tl^{2+} to $RbCl$:Tl^{2+} can reasonably be associated with an increase of the equilibrium Tl^{2+}–Cl^- distance $\Delta R_e = 3$ pm. It is worthwhile noting that this value is, as expected, positive but at the same time much smaller than $\Delta R_0 = 15$ pm corresponding to the increase experienced by the anion-cation distance of the perfect host lattice. This behaviour has been observed in the case of common impurities, where the impurity–ligand distance is only slightly dependent on the host lattice (Barriuso and Moreno 1984). As to the actual value of the equilibrium Tl^{2+}–Cl^- distance for KCl:Tl^{2+}, the results collected in table 1 indicate that R would be close to 2.80 Å, which thus implies an inwards relaxation of about 10% with respect to the cation–anion separation ($R = 3.14$ Å) of the perfect host lattice.

In table 2 the calculated energies of optical transitions for $TlBr_6^{4-}$, TlI_6^{4-} and also $TlCl_6^{4-}$ are presented. The calculations lead to a $\sim$1.7 eV red shift of CT transitions on passing from $TlCl_6^{4-}$ to TlI_6^{4-} which is very close to that observed experimentally (part I, figure 2).
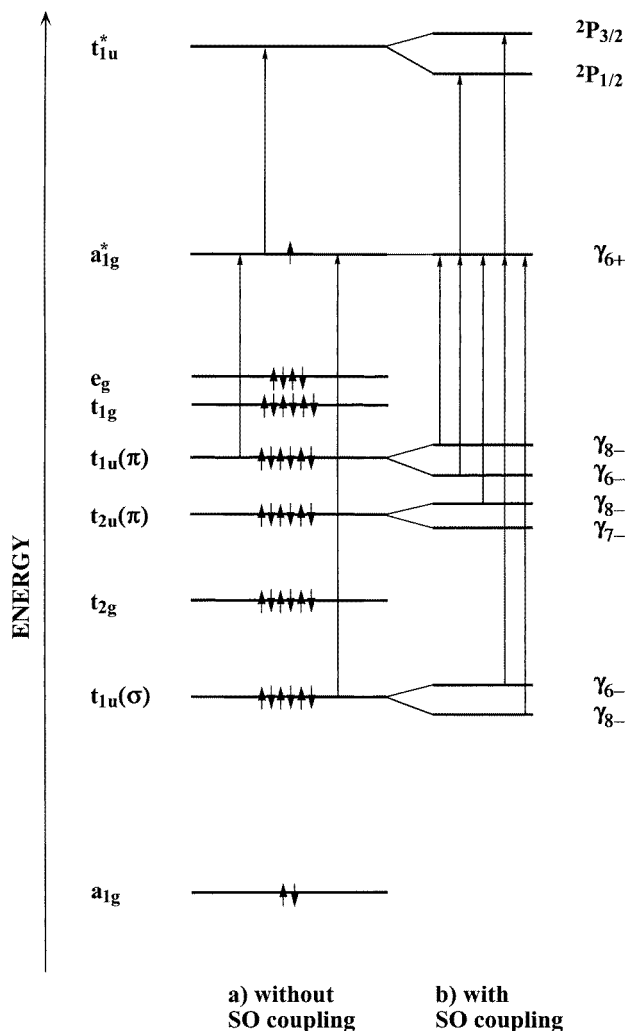
Figure 1. Molecular orbital diagram for octahedral TlX_6^{4-} units (X = Cl, Br, I) derived from the present MS–Xα calculations. In that diagram only the one-electron levels arising from the 6s and 6p levels of free Tl^{2+} and from n_{LP} levels (n_L = quantum number of the valence shell) of the six halogen ions involved in the complex are shown. The unpaired electron is located in the antibonding a_{1g}^* level and the six levels lying below are made mainly from n_{LP} levels of the ligands. In the figure the electric-dipole-allowed transitions for TlX_6^{4-} units are also shown. The expected transitions, when the spin–orbit coupling is present or absent, are both depicted. In the absence of spin–orbit coupling only the $a_{1g}^* \rightarrow t_{1u}^*$ and the two charge transfer transitions, $t_{1u}(\pi) \rightarrow a_{1g}^*$ and $t_{1u}(\sigma) \rightarrow a_{1g}^*$, are allowed, while when that coupling exists, seven transitions are permitted. Note that only the γ_{8-} component of the $t_{2u} \rightarrow a_{1g}^*$ transition becomes allowed as far as the ligand spin–orbit coupling increases.

It is worth noting that the corresponding experimental red shift for the $a_{1g}^* \rightarrow t_{1u}^*$ transition is only 0.7 eV and thus nearly half the value observed for CT transitions. This trend is also reproduced by the present calculations.

Table 1. Optical transition energies (in eV) calculated through the MS–Xα method for $TlCl_6^{4-}$ (first row) and $(TlCl_6K_{12}Cl_8)^0$ (second row) clusters at different values of the metal–ligand distance R (in Å). The results are compared to the experimental values in $KCl:Tl^{2+}$ (Delbecq *et al* 1996). In the case of the $a_{1g}^* \rightarrow t_{1u}^*$ transition the theoretical value is compared to the centre of the gravity associated with the $^2P_{1/2}$ and $^2P_{3/2}$ states. Note that the transition energies are nearly independent of the cluster size.

			R		
Transition	2.75	2.80	2.85	2.90	Experimental
$a_{1g}^* \rightarrow t_{1u}^*$	5.34	5.48	5.69	5.79	5.33
	5.24	5.55	5.74	5.85	
$t_{1u}(\pi) \rightarrow a_{1g}^*$	3.57	3.26	2.89	2.58	3.40
	3.66	3.26	2.90	2.55	
$t_{1u}(\sigma) \rightarrow a_{1g}^*$	4.50	4.11	3.68	3.31	4.22
	4.60	4.13	3.69	3.29	

Table 2. Optical transition energies, E (in eV), calculated through the MS–Xα method for $TlCl_6^{4-}$, $TlBr_6^{4-}$ and TlI_6^{4-} complexes. The value (in Å) of the metal–ligand distance R, taken for each complex, is also given. The sensitivity, dE/dR (in meV pm^{-1}), to changes of R is also reported.

		$a_{1g}^* \rightarrow t_{1u}^*$		$t_{1u}(\pi) \rightarrow a_{1g}^*$		$t_{1u}(\sigma) \rightarrow a_{1g}^*$	
	R	E	dE/dR	E	E/dR	E	dE/dR
$TlCl_6^{4-}$	2.80	5.48	30	3.26	−66	4.11	−79
$TlBr_6^{4-}$	3.00	5.36	18	2.05	−50	3.00	−64
TlI_6^{4-}	3.25	4.94	8	1.45	−37	2.40	−50

The sensitivity dE/dR of different transition energies for $TlBr_6^{4-}$ and TlI_6^{4-} is also given in table 2, and the trends are similar to those obtained for $TlCl_6^{4-}$. As a salient feature, the 6s $\rightarrow$ 6p-like transition is calculated to be less sensitive to R changes than the CT transitions. This is again in agreement with what is experimentally observed (part I, figure 2), in particular for $RbI:Tl^{2+}$ and $KI:Tl^{2+}$, where the two $^2P_{1/2}$ and $^2P_{3/2}$ components of the $a_{1g}^* \rightarrow t_{1u}^*$ transition are well observed. Therefore, the experimental dE/dR value can be used as an *additional* argument for distinguishing a CT transition from the 6s $\rightarrow$ 6p-like.

As to the electron density, the red shift undergone by the CT transitions on passing from $KCl:Tl^{2+}$ to $KI:Tl^{2+}$ should also imply an increase in the unpaired spin density on ligands. This idea is confirmed by the results on the charge distribution in the a_{1g}^* orbital given in table 3. Moreover, these results indicate that the unpaired electron is located more on the ligands than on the central ion. Also, the decrease followed by the charge on the Tl(6s) orbital along the Cl $\rightarrow$ Br $\rightarrow$ I series can be related to the decrease of the experimental hyperfine constant A. For instance, the experimental value for Tl in alkali chlorides is $A = 104$ GHz, while $A = 93$ GHz in the case of bromides. In recent experiments on Tl^{2+} in $PbCl_2$, where the co-ordination number is also six, the hyperfine constant has also been measured to be close to 100 GHz (Nistor *et al* 1995). As to the Tl(6s) charge (table 3), it decreases by about 10% on going from $TlCl_6^{4-}$ to $TlBr_6^{4-}$. This decrease is thus comparable to that experienced by A. Nevertheless, the reduction of A (part I, table 1) when passing from $KBr:Tl^{2+}$ ($A = 93$ GHz) to $KI:Tl^{2+}$ ($A = 52$ GHz) is higher than that corresponding

Table 3. Distribution of the electronic charge (in %) for the unpaired a_{1g}^* level obtained through the MS–Xα method for the indicated complexes. The value (in Å) of the metal–ligand distance R at which calculations have been carried out is also given.

	R	Tl (6s)	X (ns)	X (np)
$TlCl_6^{4-}$	2.80	39.9	7.2	52.9
$TlBr_6^{4-}$	3.00	34.1	4.4	61.5
TlI_6^{4-}	3.25	29.7	2.6	67.7

to the charge on the central ion. A clarification of this point requires a further study of the actual g factor associated with TlI_6^{4-}. A first analysis of the g factor using a perturbative scheme (Moreno 1980) suggests that g values around 2.5 are not unreasonable for TlI_6^{4-}.

It is worth noting that the $|a_{1g}^*\rangle$ wavefunction can be briefly expressed as

$$|a_{1g}^*\rangle = \alpha_M |Tl(6s)\rangle - \lambda_{p\sigma}|\phi_{p\sigma}\rangle - \lambda_s|\phi_s\rangle \tag{1}$$

where $|\phi_{p\sigma}\rangle$ and $|\phi_s\rangle$ signify linear combinations of valence $p\sigma$ and s orbitals of involved ligands. It is convenient to note that A is proportional to α_M^2 which is *higher* than the charge related to Tl(6s) because of the antibonding nature of this orbital. Therefore, the reduction experienced by A when passing from free Tl^{2+} ($A_0 = 175$ GHz) to KBr:Tl^{2+} is close to 50% which is higher than the charge reported in table 3.

Although a more detailed study of the hyperfine coupling is currently under way, polarized MS–Xα calculations already stress that for Tl^{2+} impurities the contribution to A coming from the polarization of core s levels by the unpaired electron is only $\sim$0.3% of that due to the unpaired a_{1g}^* electron alone. Therefore, at variance with what happens in the case of 3d cations (Abragam and Bleaney 1970), in the present cases the core polarization can be discarded in the analysis of the experimental hyperfine constant.

Going further into the analysis of experimental data it becomes necessary to discuss in some detail the origin of *all* bands associated with the $t_{1u}(\pi) \rightarrow a_{1g}^*$ and $t_{1u}(\sigma) \rightarrow a_{1g}^*$ transitions, as well as their MCDA sign. To this end it is crucial to consider the effect of the spin–orbit coupling. As for a p level of the central ion, one t_{1u} level leads to two levels when the spin–orbit coupling is taken into account. These levels belong to the γ_{6-} and γ_{8-} representations of the cubic double group, and in the case of the t_{1u}^* level they are often denoted as $P_{1/2}$ and $P_{3/2}$, respectively. In contrast to what happens for t_{1u}^* the splitting Δ between γ_{6-} and γ_{8-} for $t_{1u}(\pi)$ and $t_{1u}(\sigma)$ strongly depends upon the ligand spin–orbit coefficient, ξ_L.

For calculating Δ let us first formularize the z component of a $|t_{1u}\rangle$ wavefunction as

$$|t_{1u}, z\rangle = \alpha|Tl(6p_z)\rangle + \beta_\pi|\chi_{p\pi}, z\rangle + \beta_\sigma|\chi_{p\sigma}, z\rangle \tag{2}$$

where $|\chi_{p\pi}, z\rangle$ and $|\chi_{p\sigma}, z\rangle$ are linear combinations of p-ligand orbitals described in figure 2. Similar to what has been obtained for Cu^{2+} in chlorides (Barriuso *et al* 1997) the $t_{1u}(\pi)$ and $t_{1u}(\sigma)$ levels in the present cases are found to be mainly built from these ligand orbitals, while the amount of Tl(6p) admixture is small, but not negligible. As the $|\chi_{p\pi}, z\rangle$ and $|\chi_{p\sigma}, z\rangle$ LCAOs are, in principle, degenerate, both wavefunctions are strongly mixed in the two $t_{1u}(\pi)$ and $t_{1u}(\sigma)$ levels. The highest $t_{1u}(\pi)$ level is an antibonding level with respect to the *ligand–ligand* interaction and so in this level β_π and β_σ have the same sign leading to a diminution of the electronic density in the middle region between two closest ligands. The opposite happens in the case of the $t_{1u}(\sigma)$ level, which exhibits a bonding character with respect to the ligand–ligand interaction and thus $\beta_\sigma \beta_\pi$ is negative. As previously discussed
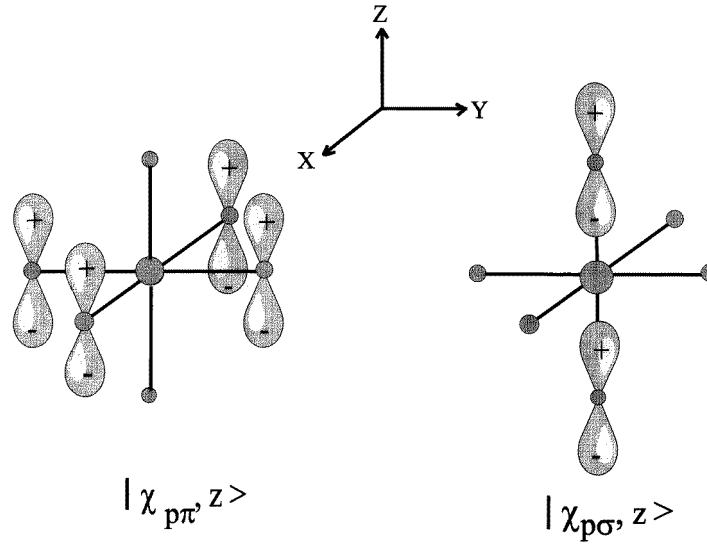
Figure 2. Pictorial description of the two linear combination of ligand p orbitals belonging to t_{1u} and transforming like z. $|\chi_{p\sigma}\rangle$ and $|\chi_{p\pi}\rangle$ involve a σ and π character, respectively, with respect to the metal–ligand interaction.

(Barriuso *et al* 1997), when the Tl(6p) admixture is switched on, it enhances the σ character of $t_{1u}(\sigma)$ and thus decreases the σ character of $t_{1u}(\pi)$. As regards the numerical values, the present calculations lead to $\alpha^2 \cong 5\%$ $\beta_\sigma\beta_\pi \cong -0.37$ for the $t_{1u}(\sigma)$ level, while $\alpha^2 \cong 1\%$, $\beta_\sigma\beta_\pi \cong 0.46$ for the $t_{1u}(\pi)$ level.

Provided that, in a first approximation, the spin–orbit operator is diagonalized within the $t_{1u}(j) \times \gamma_6$ manifold ($j = \pi, \sigma$), the value of Δ can simply be expressed as

$$\Delta = \tfrac{3}{2}\mathrm{i}\langle t_{1u}, x|T_z|t_{1u}, y\rangle \tag{3}$$

where the spin–orbit operator for an electron, h_{SO}, is given by

$$h_{SO} = \boldsymbol{T} \cdot \boldsymbol{s} \tag{4}$$

and $\boldsymbol{T}$ is an operator transforming like the orbital angular momentum, $\boldsymbol{l}$, which can be expressed (Misetich and Buch 1964, Misetich and Watson 1966) as

$$\boldsymbol{T} = \sum_k \xi(\boldsymbol{r} - \boldsymbol{R}_k)\boldsymbol{l}_k. \tag{5}$$

In (5) $\boldsymbol{l}_k$ represents the orbital angular momentum referred to the nucleus at $\boldsymbol{R}_k$ as origin and the $\xi(\boldsymbol{r} - \boldsymbol{R}_k)$ function is especially important in the vicinity of such a nucleus (Misetich and Watson 1966, Al-Mobarak and Warren 1973). Due to this fact $\xi(\boldsymbol{r} - \boldsymbol{R}_k)$ only connects two atomic orbitals, both belonging to the atom placed at $\boldsymbol{R}_k$. Taking hence into account (2)–(5) and figure 2 the expression of Δ is found to be

$$\Delta = \tfrac{3}{2}\{\alpha^2\xi_M + \xi_L(\sqrt{2}\beta_\sigma\beta_\pi + \beta_\pi^2/2)\} \tag{6}$$

where $\Delta = 3/2\xi_M$ for the case of a *free* central ion as it should be.

To estimate Δ by means of (6), $\xi_M = 1010$ meV is used for Tl, while the atomic values $\xi_L(\mathrm{Cl}) = 72$ meV, $\xi_L(\mathrm{Br}) = 300$ meV and $\xi_L(\mathrm{I}) = 628$ meV are employed for ligands (Moore 1971). The calculated values (table 4) of the splitting Δ for the two $t_{1u}(\pi)$ and

Table 4. Values of the splitting, Δ (in meV), produced by the spin–orbit coupling in the $t_{1u}(\pi)$ and $t_{1u}(\sigma)$ charge transfer levels, obtained through the present MS–Xα calculations and (6) for the indicated complexes. The value (in Å) of the metal–ligand distance R at which calculations have been carried out is also given.

	R	$t_{1u}(\pi)$	$t_{1u}(\sigma)$
$TlCl_6^{4-}$	2.80	110	30
$TlBr_6^{4-}$	3.00	450	-130
TlI_6^{4-}	3.25	920	-340

$t_{1u}(\sigma)$ levels in $TlCl_6^{4-}$ and $TlBr_6^{4-}$ reproduce the main trends displayed by the experimental splittings (part I, figure 2). It is worth stressing that for the $t_{1u}(\pi)$ level, Δ is always positive, while it can be negative for the $t_{1u}(\sigma)$ one, as a result of the $\sigma-\pi$ hybridization. The present results indicate that Δ can, in fact, be negative for the $t_{1u}(\sigma)$ level of $TlBr_6^{4-}$ and TlI_6^{4-}. This means, for instance, that the 2.55 eV and 3.05 eV peaks in $KBr:Tl^{2+}$ should be ascribed, respectively, to the γ_{8-} and γ_{6-} components of $t_{1u}(\pi)$ while the 3.57 eV and 4.0 eV peaks should be associated with the γ_{6-} and γ_{8-} components of $t_{1u}(\sigma)$, respectively.

Regarding the sign of Δ, the MCDA technique is a good tool for its *direct* measurement (Spaeth *et al* 1992). For an atomic-like s $\rightarrow$ p transition if $\Delta > 0$, the MCDA sign of the γ_{6-} component is negative, while that of the γ_{8-} component is positive (Paus 1980). In fact, the MCDA at $T = 0$ K in the γ_{6-} component is determined by the matrix element $\langle a_{1g}^*,$ $M_J = -1/2|J_-|t_{1u}^*\gamma_{6-}; M_J = 1/2\rangle$ thus giving rise to a left circular light absorption. The MCDA pattern of a normal s $\rightarrow$ p transition can be represented as $(-; +)$. Here, the first (second) part refers to the lowest (highest) energy side and a positive value in the bracket implies a positive value of the MCDA in figure 2 of part I.

In the case of CT transitions the situation is somewhat different. In fact, in a $t_{1u}(j) \rightarrow a_{1g}^*$ ($j = \pi, \sigma$) transition the electron reaches the *empty* $|a_{1g}^*, M_J = 1/2\rangle$ level and thus the γ_{6-} component is determined by the matrix element $\langle t_{1u}(j); \gamma_{6-};$ $M_J = -1/2|J_-|a_{1g}^*; M_J = 1/2\rangle$. As the $t_{1u}(j)$ levels are lying *below* a_{1g}^*, the γ_{6-} component now still appears in the *high* energy side provided $\Delta > 0$. Therefore, a $t_{1u}(j) \rightarrow a_{1g}^*$ CT transition should give rise to a $(+; -)$ MCDA pattern if $\Delta > 0$. This is *opposite* to what is found for an atomic-like s $\rightarrow$ p transition. As Δ is found to be positive for $t_{1u}(\pi)$, the two bands arising from the $t_{1u}(\pi) \rightarrow a_{1g}^*$ transition should follow that pattern.

This conclusion is consequently in agreement with what is observed for chlorides and bromides (part I, figure 2). Table 4 furthermore indicates that in the case of the chlorides the Δ value related to the $t_{1u}(\sigma)$ level is much smaller than that corresponding to $t_{1u}(\pi)$. Therefore the near absence of an MCDA signal for $KCl:Tl^{2+}$ and $RbCl:Tl^{2+}$ associated with the $t_{1u}(\sigma) \rightarrow a_{1g}^*$ transition can be reasonably be explained now. In fact, when the spin–orbit coupling is not directly seen in the absorption spectrum, the MCDA signal is just proportional to Δ (Paus 1980). The experimental results displayed in figure 2 of part I for $MBr:Tl^{2+}$ (M = K, Rb) indicate that MCDA signs in the $t_{1u}(\sigma) \rightarrow a_{1g}^*$ region follow the pattern $(-; +)$, thus confirming the negative value of Δ estimated for $TlBr_6^{4-}$ in table 4.

Let us finally discuss the MCDA spectra due to Tl^{2+} in iodides, where five and not four CT maxima are clearly seen, as was discussed in part I. When observing the experimental results on chlorides and bromides, it is reasonable to relate four of the observed maxima to transitions emerging from $t_{1u}(\pi) \rightarrow a_{1g}^*$ and $t_{1u}(\sigma) \rightarrow a_{1g}^*$. Taking into account the estimated Δ values in table 4 only one assignment is found to be reasonable. For $KI:Tl^{2+}$ that

assignment is as follows: the peaks at 1.6 eV and 2.45 eV are the γ_{8-} and γ_{6-} components related to $t_{1u}(\pi)$, while peaks at 2.8 eV and 3.43 eV are the γ_{6-} and γ_{8-} components, respectively, associated with $t_{1u}(\sigma)$. As is clearly observed in the experimental spectrum, the first couple exhibits a $(+; -)$ MCDA pattern, while the second one exhibits an inverse pattern in agreement with the negative Δ value given in table 4.

After this analysis it becomes clear that the peak observed at 2.07 eV in KI:Tl^{2+} and 2.03 eV in RbI:Tl^{2+} is the *new* peak, which cannot be understood on the basis of $t_{1u}(j) \to a^*_{1g}$ ($j = \pi, \sigma$) transitions split off by the action of the spin–orbit coupling. As the tagged MCDA spectra stress that the seven peaks seen for MI:Tl^{2+} (M = K, Rb) are *all* related to a Tl^{2+} impurity in a local cubic symmetry, it is reasonable to firstly search for an explanation for the new peak on the basis of unperturbed TlI$_6^{4-}$ units. Bearing in mind that in the full series the new peak is clearly observed only in the iodides, it could reasonably be associated with *another* manifestation of the ligand spin–orbit coupling.

When looking at the molecular orbitals built from the valence p levels of six ligands (Ballhausen and Gray 1965), only one *odd* linear combination is found besides the $|\chi_{p\pi}\rangle$ and $|\chi_{p\sigma}\rangle$ combination described in figure 2. Such an orbital is purely non-bonding with respect to the metal–ligand interaction and transforms like t_{2u} instead of t_{1u}. Although the parity-allowed $t_{2u} \to a^*_{1g}$ transition is strictly forbidden in the absence of a spin–orbit coupling, it is no longer true when switching on such an interaction (figure 1). Actually, a t_{2u} level gives rise to γ_{7-} and γ_{8-} levels when the spin–orbit coupling is taken into account. Therefore, *only one* of these components would give rise to an electric-dipole-allowed transition and so the number of permitted charge transfer transitions would in fact be five and not four.

For supporting this attractive possibility it now becomes necessary to observe where the t_{2u} level is located with respect to $t_{1u}(\pi)$ and $t_{1u}(\sigma)$. The present calculations indicate (figure 1) that t_{2u} is always located *just below* $t_{1u}(\pi)$, the separation between them being smaller than ~ 0.15 eV. This separation remains when calculating the corresponding transitions to the a^*_{1g} level. The $t_{2u}(\gamma_{8-}) \to a^*_{1g}$ transition is hence suggested to be located a little above the $t_{1u}(\pi; \gamma_{8-}) \to a^*_{1g}$ one from which it borrows oscillator strength if ξ_L increases.

On the other hand, as the calculated separation between $t_{1u}(\pi)$ and t_{2u} is never much higher than the involved ligand spin–orbit coefficient, ξ_L, the allowed $t_{2u}(\gamma_{8-}) \to a^*_{1g}$ transition would *also* appear to be present in the case of bromides and chlorides. This idea can now explain the puzzling asymmetry displayed by the MCDA signal in the $t_{1u}(\pi) \to a^*_{1g}$ region (part I, figure 2), where the intensity of the $t_{1u}(\pi, \gamma_{6-})$ peak is clearly smaller than that due to $t_{1u}(\pi, \gamma_{8-})$. This effect could result from the *simultaneous* presence of the $t_{2u}(\gamma_{8-}) \to a^*_{1g}$ positive MCDA signal in the high energy side of the $t_{1u}(\pi) \to a^*_{1g}$ MCDA band. Although this explanation seems reasonable, a deeper analysis of the influence of spin–orbit coupling on charge transfer levels is currently being carried out.

Apart from this relevant aspect and a more detailed study of the hyperfine constant and g factor, other points deserving further investigation are: (i) the nature of the t^*_{1u} level, where a hybridization with lowest levels of the conduction band of the host lattice appears to play an important role; (ii) the correct value of the equilibrium distance between the Tl^{2+} impurity and nearest anions.

To clarify these points, calculations on 81 atom clusters using density functional theory as implemented in the ADF program system (Baerends and Ellis 1973, te Velde and Baerends 1992) have been initiated. In the first calculation a value $R_e = 2.75$ Å for the equilibrium distance in KCl:Tl^{2+} has been obtained. Thus the existence of an important inwards lattice relaxation indirectly obtained through the present work appears to be more strongly supported. Further work along this line is now under way.

Acknowledgments

References

Abragam A and Bleaney B 1970 *Electron Paramagnetic Resonance of Transition Ions* (Oxford: Oxford University Press) p 702
Al-Mobarak R and Warren K D 1973 *Chem. Phys. Lett.* **21** 513
Aramburu J A, Barriuso M T and Moreno M 1996 *J. Phys.: Condens. Matter* **8** 6901
Aramburu J A and Moreno M 1997 *Phys. Rev.* B **56** 604
Aramburu J A, Moreno M and Barriuso M T 1992 *J. Phys.: Condens. Matter* **4** 9089
Baerends E J and Ellis D E 1973 *Chem. Phys.* **2** 42
Ballhausen C J and Gray H B 1965 *Molecular Orbital Theory* (New York: Benjamin) p 103
Barriuso M T, Aramburu J A, Daul C and Moreno M 1997 *Int. J. Quant. Chem.* **61** 563
Barriuso M T and Moreno M 1984 *Phys. Rev.* B **29** 3623
Bramanti D, Mancini M and Ranfagni A 1971 *Phys. Rev.* B **3** 3670
Cabria I, Barriuso M T, Aramburu J A and Moreno M 1997 *Int. J. Quant. Chem.* **61** 627
Delbecq C J, Ghosh A K and Yuster P H 1966 *Phys. Rev.* **151** 599
Jørgensen C K 1970 *Prog. Inorg. Chem.* **12** 101
Misetich A A and Buch T 1964 *J. Chem. Phys.* **41** 2524
Misetich A A and Watson R E 1966 *Phys. Rev.* **143** 335
Moore C E 1971 *Atomic Energy Levels* National Bureau of Standards
Moreno M 1979 *J. Phys. C: Solid State Phys.* **12** L921
——1980 *Chem. Phys. Lett.* **76** 597
Nistor S V, Goovaerts E and Schoemaker D 1995 *Solid State Commun.* **96** 491
Nistor S V, Schoemaker D and Ursu I 1994 *Phys. Status Solidi* b **185** 9
Norman J G 1976 *Mol. Phys.* **31** 1191
Paus H J 1980 *Habilitationsschrift* Universität Stuttgart
Rogulis U, Dietze C, Pawlik Th, Hangleiter Th and Spaeth J-M 1996 *J. Appl. Phys.* **80** 2430
Rogulis U, Spaeth J-M, Cabria I, Moreno M, Aramburu J A and Barriuso M T 1998 *J. Phys.: Condens. Matter* **10** 6473
Sakurai J J 1967 *Advanced Quantum Mechanics* (Reading, MA: Addison-Wesley)
Schwarz K 1972 *Phys. Rev.* B **5** 2466
Slater J C 1974 *Quantum Theory of Molecules and Solids* vol 4 (New York: McGraw-Hill)
Spaeth J-M, Niklas J R and Bartram R H 1992 *Structural Analysis of Point Defects in Solids, (Springer Series of Solid State Sciences 43)* (Berlin: Springer)
te Velde G and Baerends E J 1992 *J. Comput. Phys.* **99** 84
Wood J H and Boring A M 1978 *Phys. Rev.* B **18** 2701